

**Manipulation of fullerene-induced impurity states in carbon peapods**

Mao-Hua Du and Hai-Ping Cheng

*Department of Physics and Quantum Theory Project, University of Florida, Gainesville, Florida 32611, USA*

(Received 22 April 2003; published 11 September 2003)

Electronic structures of several semiconducting and metallic carbon peapods have been studied using density functional theory. We have systematically investigated the effects of two key factors, the tube diameter and the type of the encaged metal atom inside  $C_{60}$ , on the energy level and the electron occupation number of  $C_{60}$ -induced impurity states in semiconducting peapods. The manipulation of these impurity states controls the type of the majority carrier ( $p$  or  $n$ ) and the carrier density of a semiconducting peapod. In addition, the possibility of superconductivity of potassium-doped peapods has been discussed.

DOI: 10.1103/PhysRevB.68.113402

PACS number(s): 71.20.Tx, 73.20.At, 73.22.-f

Since the discoveries of carbon fullerenes in 1985<sup>1</sup> and nanotubes in 1991,<sup>2</sup> these two carbon allotropes have attracted considerable attention in the scientific community because of their unique structures and properties. A carbon nanotube can be metallic or semiconducting, depending on its chiral vector  $(n, m)$ . Chemical doping can further modify electrical properties of carbon nanotubes, for instance, potassium or bromine doping enhances conductivity.<sup>3</sup> Alkali metal and alkaline-earth intercalated fullerenes have also been studied extensively because of their complex phase diagram and superconductivity at temperatures surpassed only by the high- $T_c$  cuprates.<sup>4,5</sup>

The empty spaces inside carbon fullerenes and nanotubes provide the possibility to modify their properties by inserting atoms or molecules into these hollow spaces. A large number of species have been experimentally observed to sit stably inside fullerene cages<sup>6,7,8</sup> or nanotubes.<sup>9,10,11</sup> Theoretical calculations have revealed the details of the energetics and electronic structure of fullerene and nanotube endohedral complexes.<sup>12,13,14,15,16</sup> Recently, Smith *et al.* have successfully encapsulated  $C_{60}$  molecules in single-wall carbon nanotubes (SWNTs) (Ref. 17) and achieved a high-yield synthesis of such “peapods.”<sup>18</sup> More complex metallofullerene peapods [ $(Gd@C_{82})_n@SWNTs$ ,  $(La_2@C_{80})_n@SWNTs$ , etc.] have also been identified in transmission electron microscopy images.<sup>19,20,21</sup>

Encapsulation of fullerenes and metallofullerenes inside nanotubes enables the development of a new class of hybrid materials, which exhibits many interesting properties. The electrical resistivity, thermopower and thermal conductivity of peapods are different from those of empty SWNTs.<sup>19,22,23</sup> Scanning tunneling microscopy (STM) studies show the spatially varied local density of states (LDOS) in  $C_{60}@SWNT$  (Ref. 24) and the spatial modulation of energy band gap in  $(Gd@C_{82})_n@SWNT$ .<sup>25</sup> A temperature-induced change from  $p$  to  $n$  conduction in  $(Dy@C_{82})_n@SWNT$  (Ref. 26) and ambipolar field-effect transistor behavior of  $(Gd@C_{82})_n@SWNT$  (Ref. 27) have also been reported. An encapsulated  $C_{60}$  chain may also show superconductivity upon alkaline doping, in analogy with fullerene intercalation compounds.<sup>4,5</sup> In order to fully understand how the different encapsulants affect physical properties of their host nanotubes, substantial theoretical studies of the electronic structures of peapods are highly desired.

In this paper, we report our work on electronic structures of several semiconducting and metallic nanopeapods. We manipulate the  $C_{60}$  induced impurity states inside the band gap of the host semiconducting nanotubes by controlling the distance between the tube and  $C_{60}$  and the type of the encaged metal atom inside  $C_{60}$ . The states hybridization and the effects of density and orientation of encapsulated  $C_{60}$  molecules have been analyzed. In addition, we discuss the possibility of superconductivity of potassium-doped peapods.

The electronic structure calculations are performed using density functional theory with the local density approximation. The electron-ion interactions are described by ultrasoft pseudopotentials.<sup>28</sup> The valence wave functions are expanded in a plane-wave basis set with an energy cutoff of 286 eV, which has been tested and found to give a good energy convergence. The supercell is chosen such that the distance between adjacent nanotube walls is longer than 6.7 Å. We use two  $k$  points in the irreducible Brillouin zone. All calculations are performed using the Vienna *ab initio* simulation package.<sup>29</sup>

As the model systems for our theoretical investigation, we choose (16, 0), (17, 0), (19, 0), and (10, 10) nanotubes and their corresponding fullerene or metallofullerene encapsulated peapods. A commensurability condition is imposed between the periodicity of the nanotube and that of the  $C_{60}$  chain. The optimized lattice parameter  $c$  is 9.79 Å for the (10, 10) nanotube, and 12.68 Å for all zigzag tubes. In order to study (17, 0) peapods with different  $C_{60}$  intermolecular distances, we use two different lattice lengths (triple and quintuple periodicity of a zigzag nanotube) for the (17, 0) peapod. These two different unit cells contain one and two  $C_{60}$  molecules with optimized lattice parameters of 12.68 and 21.14 Å, respectively. (17, 0) peapods with smaller and larger lattice parameters are labeled as  $(17,0)^a$  and  $(17,0)^b$  peapods in the rest of the paper.

In an isolated  $C_{60}$  molecule, there is a threefold degenerate lowest unoccupied  $t_{1u}$  state. Figure 1 shows the electronic band structures of the  $C_{60}@ (17,0)$  peapod. The band structure of the (10, 10) peapod obtained in this work is similar to a previous result.<sup>30</sup> From Figs. 1(b) and 1(c), the (17, 0) peapod remains a semiconductor. In the  $(17,0)^a$  peapod, the flat energy band inside band gap is derived from the  $t_{1u}$  state of  $C_{60}$ . There is nearly no energy dispersion for the

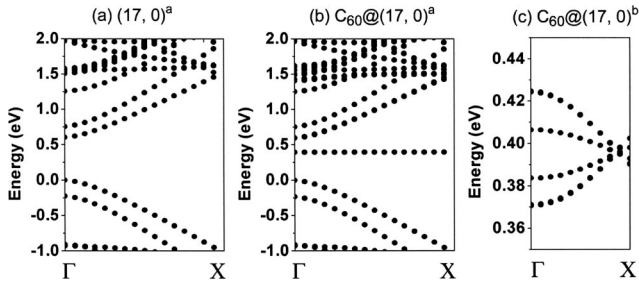


FIG. 1. Energy band structures of empty and  $C_{60}$  encapsulated  $(17, 0)$  nanotube. (a) Empty nanotube. (b)  $C_{60}@ (17, 0)^a$ . (c)  $C_{60}@ (17, 0)^b$ . In (c), only  $C_{60} t_{1u}$ -derived impurity bands inside the band gap are shown. Note the size of the first-Brillouin zone for  $(17, 0)^b$  peapod is three-fifths of that for  $(17, 0)^a$  peapod because of its larger unit cell.

$t_{1u}$ -derived band because of the long center-to-center distance  $d_c$  between two  $C_{60}$  molecules, while there is a very small energy dispersion in the  $(17, 0)^b$  peapod. When  $d_c$  is large, the  $C_{60}$  chain is broken and not conductive, so that the  $t_{1u}$ -derived states behave as impurity states [see Fig. 1(b)] and carriers are distributed on the nanotube wall. When  $d_c$  decreases, these impurity states become impurity bands [see Fig. 1(c)] and conductive, resulting in most hole carriers distributed on the nanotube wall and most electron carriers on the  $C_{60}$  chain at a temperature not high enough to make the intrinsic carrier concentration dominant.

The small  $t_{1u}$  bandwidth in the  $(17, 0)^b$  peapod is not only due to the relatively larger  $d_c$ , but also due to the ordered orientation of the  $C_{60}$  molecules inside the nanotube. On rotating one of the two  $C_{60}$  molecules in the unit cell of the  $(17, 0)^b$  peapod around the tube axis by  $180^\circ$ , we find a doubled  $t_{1u}$  bandwidth and a reduction of the  $t_{1u}$  density of states peak by about 20%, while the total energy essentially remains the same. If  $d_c$  is about 10 Å, as found in experiment, and taking into account the random orientation of  $C_{60}$  molecules at room temperature, we expect a bigger  $t_{1u}$  bandwidth than that shown in Fig. 1(c).

While  $d_c$  and the orientation of  $C_{60}$  molecules largely determine the  $t_{1u}$  band dispersion, the space between  $C_{60}$  and the nanotube wall is a key factor for the energy levels of  $t_{1u}$ -derived states. Our calculations show that the energy levels of  $t_{1u}$ -derived states are about two-thirds of the band-gap (0.6 eV) above the top of the valence band ( $E_v$ ) in  $C_{60}@ (17, 0)$  [see Fig. 1(b)], while they are inside conduction band in  $C_{60}@ (16, 0)$ , and about one-third of the band gap (0.48 eV) above  $E_v$  in  $C_{60}@ (19, 0)$  (not shown). The diameters of (16, 0), (17, 0) and (19, 0) nanotubes are 12.48, 13.26, and 14.80 Å, respectively. It was reported in a recent paper that energy levels of  $t_{1u}$ -derived states are two-fifths of the band gap (0.5 eV) above  $E_v$  in  $C_{60}@ (14, 7)$ .<sup>31</sup> The diameter of the (14, 7) nanotube is 14.48 Å. It is evident that the  $t_{1u}$ -derived states shift down toward the top of the valence band as the tube diameter increases from 12.48 to 14.80 Å. The similar trend has also been found in metallic nanotubes.<sup>30</sup>

Figure 2(a) shows the calculated LDOS of the nanotube wall along the axis of the  $(17, 0)^a$  peapod. Although the total

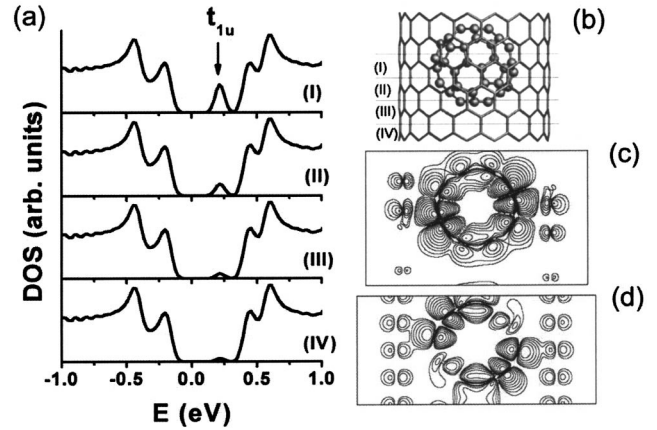


FIG. 2. The density of states projected on the nanotube wall in slices (I), (II), (III), and (IV). The sliced nanotube is shown in (b). Contour maps of the charge distribution of the lowest  $t_{1u}$ -derived energy band are shown for (c) a  $(17, 0)^a$  semiconducting peapod and (d) a  $(10, 10)$  metallic peapod. Each contour represents twice/half of the density of the neighboring line.

DOS is only projected on the nanotube, the feature from the  $C_{60} t_{1u}$  state still appears in the LDOS of the nanotube wall and gradually disappears when the distance to the center of the  $C_{60}$  molecule increases. This feature is the signature of the hybridization of the  $\pi$  states on the tube and the buckyball. This result is consistent with a recent STM study on the semiconducting peapod.<sup>24</sup> An analysis of hybridized  $t_{1u}$  wave functions shows that they are distributed on both  $C_{60}$  molecules and the tube wall and spatially varied [see Figs. 2(c) and 2(d)]. Also, they are more localized around the  $C_{60}$  molecule in the semiconducting peapod than in the metallic peapod, which suggests that it would be relatively more difficult for STM to image the spatial variation of the LDOS in a metallic peapod.

Encapsulated fullerenes or other species inside a semiconducting nanotube can be treated as impurities, whose chemical properties have an important influence on the electronic properties of the host semiconducting nanotube. In principle, a semiconducting peapod can be of  $p$  or  $n$  type, depending on whether the encapsulants are electron acceptors or donors.

$C_{60}$  has a high electron affinity and thus is an electron acceptor. It is clear from the band structure of  $C_{60}@ (17, 0)$  [Fig. 1(b)] that  $C_{60} t_{1u}$ -derived states are deep acceptor states. Encaging a metal atom inside a  $C_{60}$  molecule can change the electron affinity of the molecule and result in a change of the impurity energy level inside the band gap of the  $(17, 0)$  nanotube. Figures 3(a)–3(d) show the band structures of three metallofullerene peapods [ $K@C_{60}@ (17, 0)^a$ ,  $Ca@C_{60}@ (17, 0)^a$ , and  $Y@C_{60}@ (17, 0)^a$ ]. (We have performed the spin-polarized calculation for the  $Y@C_{60}@ (17, 0)^a$ , and found one electron spin per  $C_{60}$  molecule.) The encaged K, Ca, and Y atoms transfer about one, two, and three electrons to the  $C_{60}$  cage, respectively, as estimated by counting the electron occupation numbers of  $t_{1u}$ -derived states. The energy levels of  $t_{1u}$ -derived states in  $K@C_{60}@ (17, 0)^a$  [Fig. 3(a)] are about 0.1 eV lower than those in  $C_{60}@ (17, 0)^a$  [Fig. 1(b)]. As the charge states of the

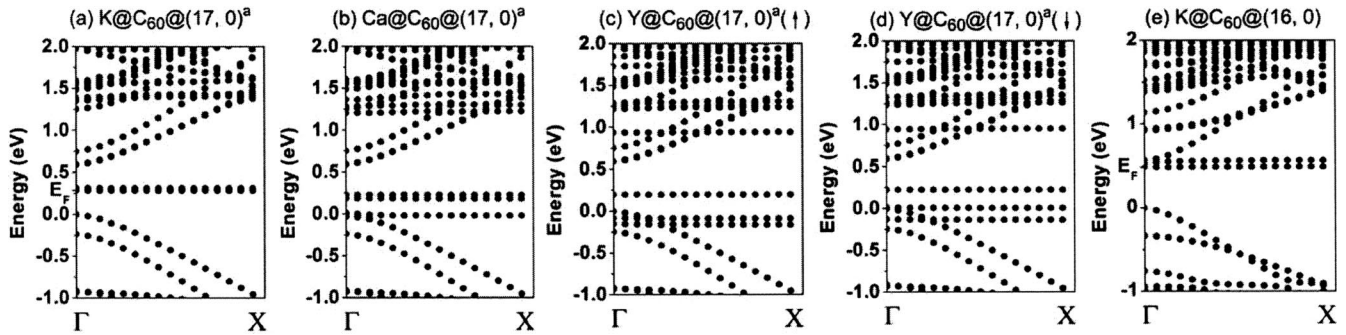


FIG. 3. Energy band structures of (a)  $\text{K@C}_{60}@(17,0)^a$ , (b)  $\text{Ca@C}_{60}@(17,0)^a$ , (c)  $\text{Y@C}_{60}@(17,0)^a$  (spin-up), (d)  $\text{Y@C}_{60}@(17,0)^a$  (spin-down), and (e)  $\text{K@C}_{60}@(16,0)$ . The origins of the energies are set at the top of the valence band ( $E_v$ ). The Fermi level  $E_F$  is indicated in (a) and (e), and equal to  $E_v$  in other figures. In (d), one of the  $t_{1u}$  derived states is a shallow acceptor state slightly above  $E_v$ .

encaged ions change from +1 and +2 to +3 (the whole system is neutral), three  $t_{1u}$ -derived energy levels downshift toward the valence band, which implies an easier electron transfer from nanotube to encapsulated  $\text{C}_{60}$ s. The experimentally measured electron affinity of  $\text{C}_{60}$  is 2.667 eV.<sup>32</sup> Our calculated electron affinities for  $\text{C}_{60}$  and  $\text{K@C}_{60}$  are 2.69 and 2.87 eV, respectively.<sup>33</sup> It has been found experimentally that metallofullerenes usually have higher electron affinity than empty  $\text{C}_{60}$ .<sup>34</sup> Therefore,  $\text{K@C}_{60}$ ,  $\text{Ca@C}_{60}$  and  $\text{Y@C}_{60}$  are better electron acceptors than empty  $\text{C}_{60}$ , which results in a downshift of  $\text{C}_{60}$   $t_{1u}$ -derived states toward the valence band upon encaging these metal atoms. As we already discussed, decreasing the tube-fullerene distance can raise the energy levels of  $t_{1u}$ -derived states. Figure 3(e) shows the band structure of  $\text{K@C}_{60}@(16,0)$ . The partially occupied  $t_{1u}$  states are below and near the bottom of the conduction band ( $E_c$ ). According to the band structures shown in Figs. 3(c)–3(e),  $\text{Y@C}_{60}@(17,0)$  is a  $p$ -type semiconductor and  $\text{K@C}_{60}@(16,0)$  is an  $n$ -type semiconductor. Apparently, the tube diameter and the type of the encaged metal atom are two key factors that determine the energy level and the electron occupation number of impurity states inside the band gap of the host semiconducting nanotube.

In analogy with the alkali-intercalated  $\text{C}_{60}$  crystal, a doped  $\text{C}_{60}$  chain may show superconductivity if the narrow  $t_{1u}$  band is nearly half filled. We encapsulate potassium atoms in the interstitial space between  $\text{C}_{60}$  and nanotube wall (Fig. 4). Electrons transfer from K atoms to both  $\text{C}_{60}$  molecules and the nanotube. In  $\text{K}_x\text{C}_{60}@(17,0)$  peapods,  $t_{1u}$ -derived bands and  $E_F$  are both shifted into the conduction band. Figure 5 shows the DOSs [ $N(E)$ ] of  $\text{K}_3\text{C}_{60}@(10,10)$  and  $(\text{K}_3\text{C}_{60})_2@(17,0)^b$ . The  $N(E_F)$  per  $\text{C}_{60}$  in either the (10, 10) or (17,0)<sup>b</sup> peapod is high and comparable to that of the  $\text{K}_3\text{C}_{60}$  crystal in the superconducting phase (about 7.2 states/eV spin).<sup>5</sup> [Note that there are two  $\text{C}_{60}$  molecules in the (17,0)<sup>b</sup> peapod, and the  $N(E_F)$  per  $\text{C}_{60}$  in the (17,0)<sup>b</sup> peapod is higher than that in the (10, 10) peapod due to the relatively larger  $\text{C}_{60}$  intermolecular distance in the (17,0)<sup>b</sup> peapod.] Thus, the critical temperature ( $T_c$ ) for alkali-doped peapods may also be comparable to or even higher than that for the alkali-intercalated  $\text{C}_{60}$  crystal. On the other hand, the lattice distortion of the  $\text{C}_{60}$  chain due to the weak  $\text{C}_{60}$ - $\text{C}_{60}$  interaction and the incommensurate charge filling of the  $\text{C}_{60}$

molecules due to the alkali atom vacancies are generally expected. How these problems affect the properties of peapods is still an open question. The future studies on the structural and phase transformation in these dimensionally constrained systems would be very interesting.

Finally, we discuss the consequence of encapsulating other types of metallofullerenes inside a semiconducting nanotube. There are many types of endohedral metallofullerenes that have been synthesized in larger quantity and with a higher purification than  $\text{M@C}_{60}$ . They have different chemical and electronic properties, depending on the fullerene size, the type, and the number of metal atoms encaged.<sup>8,12</sup> For example,  $\text{C}_{82}$  has a higher first electron affinity than  $\text{C}_{60}$  and its lowest unoccupied molecular orbital (LUMO) is nondegenerate in contrast to  $\text{C}_{60}$ . If  $\text{M@C}_{82}$  has a charge state of  $\text{M}^{3+}\text{C}_{82}^{3-}$ , the energy level of the singly occupied LUMO+1 will determine whether the peapod is a  $p$ - or  $n$ -type semiconductor. The space between  $\text{C}_{82}$  and the nanotube wall is expected to play a key role in determining the energy levels of the LUMO and LUMO+1 of  $\text{C}_{82}$ . In general, the tube-fullerene distance and the chemical properties (electron affinity and charge state) of the encapsulated metallofullerenes determine the energy level and the electron occupation number of the fullerene-induced impurity states inside the band gap. A manipulation of these impurity states enables us to find a series of semiconducting peapods with

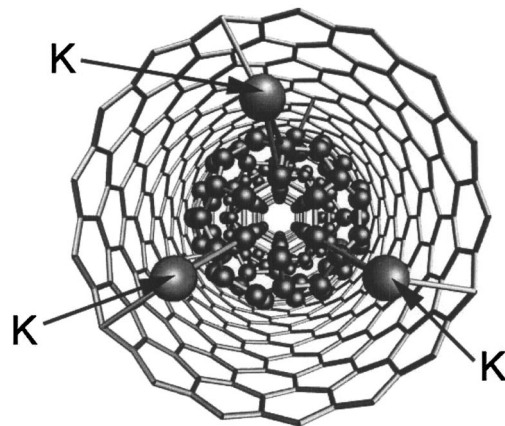


FIG. 4. The geometry of  $\text{K}_3\text{C}_{60}@(17,0)$ .

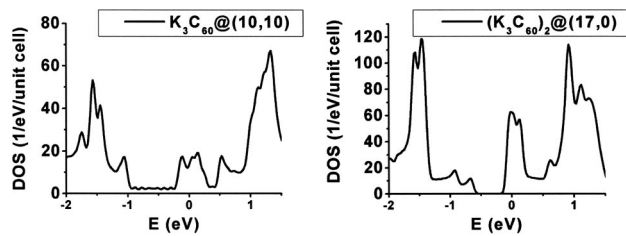


FIG. 5. The density of states of (a)  $K_3C_{60}@ (10,10)$  and (b)  $K_3C_{60}@ (17,0)$ <sup>b</sup>.

Fermi levels ranging from the valence band to the conduction band, and consequently to control the type of the majority carrier ( $p$  or  $n$ ) and the carrier density of semiconducting peapods. The family of endohedral metallofullerenes ( $M_x^{n+}@C_{2y}^{n-}$ ) behaves like a superatom with tunable size and

chemical properties. Such a large family of metallofullerenes provides us an opportunity to fine tune the electronic properties of semiconducting nanotubes to desired conditions.

In summary, we have studied electronic structures of several carbon nanotube peapods. The encapsulated fullerenes induce impurity states in semiconducting peapods. We can manipulate these impurity states to desired conditions by controlling the tube-fullerene distance and the type of the engaged metal atoms. K doping of the peapod significantly increases the DOS at  $E_F$  and makes the K-doped peapod a candidate superconductor. These findings give insights into the stable doping of the semiconducting nanotubes, and the control of the electronic properties of complex nanoscale materials.

This work was supported by Department of Energy under Contract No. DE-FG02-02ER45995.

- <sup>1</sup>H. W. Kroto, J. R. Heath, S. C. O'Brien, R. F. Curl, and R. E. Smalley, *Nature (London)* **318**, 162 (1985).
- <sup>2</sup>S. Iijima, *Nature (London)* **354**, 56 (1991).
- <sup>3</sup>R. S. Lee, H. J. Kim, J. E. Fischer, A. Thess, and R. E. Smalley, *Nature (London)* **388**, 17 (1997).
- <sup>4</sup>T. Yildirim, O. Zhou, and J. E. Fischer, in *The Physics of Fullerene-Based and Fullerene-Related Materials*, edited by W. Andreoni (Kluwer, Dordrecht, 2000).
- <sup>5</sup>O. Gunnarsson, *Rev. Mod. Phys.* **69**, 575 (1997).
- <sup>6</sup>D. S. Bethune *et al.*, *Nature (London)* **366**, 123 (1993).
- <sup>7</sup>S. Stevenson *et al.*, *Nature (London)* **401**, 55 (1999).
- <sup>8</sup>H. Shinohara, *Rep. Prog. Phys.* **63**, 843 (2000).
- <sup>9</sup>X. Fan *et al.*, *Phys. Rev. Lett.* **84**, 4621 (2000).
- <sup>10</sup>I. Mukhopadhyay *et al.*, *Physica B* **323**, 130 (2002).
- <sup>11</sup>H. Shimoda *et al.*, *Physica B* **323**, 133 (2002).
- <sup>12</sup>J. Cioslowski, *Electronic Structure Calculations on Fullerenes and Their Derivatives* (Oxford University Press, New York, 1995).
- <sup>13</sup>Y. S. Li and D. Tománek, *Chem. Phys. Lett.* **221**, 453 (1994); D. Tománek and Y. S. Li, *ibid.* **243**, 42 (1995).
- <sup>14</sup>K. Kobayashi and S. Nagase, *Chem. Phys. Lett.* **262**, 227 (1996); **282**, 325 (1998).
- <sup>15</sup>Y. Miyamoto *et al.*, *Phys. Rev. Lett.* **74**, 2993 (1995).
- <sup>16</sup>T. Miyake and S. Saito, *Phys. Rev. B* **65**, 165419 (2002).
- <sup>17</sup>B. W. Smith, M. Monthieux, and D. E. Luzzi, *Nature (London)* **396**, 323 (1998).
- <sup>18</sup>B. W. Smith *et al.*, *J. Appl. Phys.* **91**, 9333 (2002).
- <sup>19</sup>K. Hirahara *et al.*, *Phys. Rev. Lett.* **85**, 5384 (2000).
- <sup>20</sup>B. W. Smith, D. E. Luzzi, and Y. Achiba, *Chem. Phys. Lett.* **331**, 137 (2000).
- <sup>21</sup>K. Suenaga *et al.*, *Science* **290**, 2280 (2000).
- <sup>22</sup>J. Vavro *et al.*, *Appl. Phys. Lett.* **80**, 1450 (2002).
- <sup>23</sup>T. Pichler, H. Kuzmany, H. Kataura, and Y. Achiba, *Phys. Rev. Lett.* **87**, 267401 (2001).
- <sup>24</sup>D. J. Hornbaker *et al.*, *Science* **295**, 828 (2002).
- <sup>25</sup>J. Lee *et al.*, *Nature (London)* **415**, 1005 (2002).
- <sup>26</sup>P. W. Chiu *et al.*, *Appl. Phys. Lett.* **79**, 3845 (2001).
- <sup>27</sup>T. Shimada *et al.*, *Appl. Phys. Lett.* **81**, 4067 (2002).
- <sup>28</sup>D. Vanderbilt, *Phys. Rev. B* **41**, 7892 (1990).
- <sup>29</sup>G. Kresse and J. Furthmuller, *Comput. Mater. Sci.* **6**, 15 (1996); *Phys. Rev. B* **54**, 11169 (1996).
- <sup>30</sup>S. Okada, S. Saito, and A. Oshiyama, *Phys. Rev. Lett.* **86**, 3835 (2001).
- <sup>31</sup>T. Miyake and S. Saito, *Solid State Commun.* **125**, 201 (2003).
- <sup>32</sup>C. Brink *et al.*, *Chem. Phys. Lett.* **233**, 52 (1995).
- <sup>33</sup>We have used the Troullier-Martins pseudopotential and the Perdew-Burke-Ernzerhof (PBE) exchange-correlation potential for electron affinity calculations. For details of the method, see R. N. Barnett and U. Landman, *Phys. Rev. B* **48**, 2081 (1993).
- <sup>34</sup>O. V. Boltalina, I. N. Ioffe, I. D. Sorokin, and L. N. Sidorov, *J. Phys. Chem. A* **101**, 9561 (1997).